BIOPHYSICAL STUDIES ON NONCANONICAL MEMBRANE LIPIDS USING SYNTHETIC CHEMICAL TOOLS

A THESIS SUBMITTED TO THE DEPARTMENT OF CHEMISTRY
OF STANFORD UNIVERSITY
IN PARTIAL FULFILLMENT OF THE REQUIREMENTS
FOR THE DEGREE OF
MASTER OF SCIENCE

STEVEN ROBERT SHUKEN
JUNE 2018

Table of Contents

1. A hydrozirconation-carbozirconation cyclization approach to trans-1,3-disubstituted cyclopentanes en route to archaeal tetraether lipids.

Life on Earth is categorized into three domains: eukaryotes (such as animals), bacteria, and archaea. Archaea are single-celled organisms known for their ability to survive in extreme circumstances, such as temperatures as high as 122 degrees Celsius, highly acidic environments (pH < 2), and extremely high salt concentrations ([NaCl] > 2.5M).

Part of what makes an archaeum distinct is its cell membrane, which is made of lipid molecules very different from those of eukaryotes and bacteria. The significance of archaeal lipid structure, especially in effects on membrane properties, is poorly understood. This is largely because culturing archaea in the laboratory is difficult, and extracting lipids from culture or natural samples rarely results in a useful quantity of a pure lipid of a single structure. This is of concern because archaeal lipids are critical to mysterious biological processes still being explored in these intriguing organisms, and also because archaeal lipids are a very promising alternative to relatively unstable conventional phospholipid bilayer liposomes in *in vivo* delivery of drugs and diagnostics.

In order to address this, the Burns lab has established a program in which we synthesize different archaeal lipid structures and conduct biophysical and pharmacological experiments on liposomes and films constructed from them. Since the structures have many stereocenters and nearly zero functional groups, and since our applications will demand ample material (and thus high-yielding routes that minimize functional group introduction/removal steps), I was tasked with the development of a strategy whereby we can construct stereocenter-bearing hydrocarbons/carbocycles without involving traditional functional group manipulation. I investigated approaches to stereoselective cyclopentane synthesis (a long-standing problem in organic synthesis in itself) via radical, carbocationic, and organometallic mechanisms, with varying degrees of success. The most advanced result to come from this work is shown in Scheme 1. Future work will focus on zirconocene derivative design in order to optimize yield and stereoselectivity.

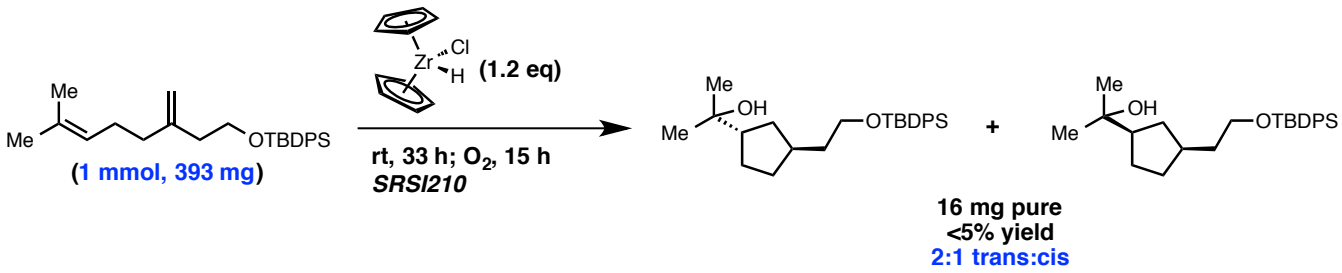

Scheme 1. Synthesis of a 1,3-disubstituted cyclopentane using a hydrozirconation-carbozirconation cyclization approach.

2. Studies on the self-assembly of fully synthetic and isolated natural danicalipin A.

Introduction

Chlorosulfolipids are a class of algal lipids with highly unusual structures.[1] Lipids that form the basis of most eukaryotic and bacterial membranes have the general architecture shown in Figure 1, with one hydrophilic head and two hydrophobic tails. Membrane chlorosulfolipids, the prototypical example being danicalipin A (Figure 2), contain a single linear alkyl chain of 22 or 24 carbons with sulfate esters bound at C1 and C14 (or C15) as well as 0 to 6 chlorine atoms.[2] Such lipids occur in varying quantities in at least 15 algal species.[3] *Ochromonas danica*, a golden-brown algal flagellate species found in acidic bogs, has a uniquely high quantity of chlorosulfolipids: chlorosulfolipids were found to make up 91% of the polar lipid content in isolated *O. danica* flagellar membranes by quantitative autoradiography.[4] Considering the 1.3:1 ratio of lipid:protein by weight in these isolates and the complete absence of phospholipids, a structural role for chlorosulfolipids must be considered.[5] In analogy to the canonical phospholipid bilayer, one may consider a parallel packing pattern, or alternatively a "hairpin" structure in which the secondary sulfate is close in space to the primary sulfate (Figure 2) although doubt has been cast on this theory considering the theoretical steric demand of the hairpin arrangement.[5]

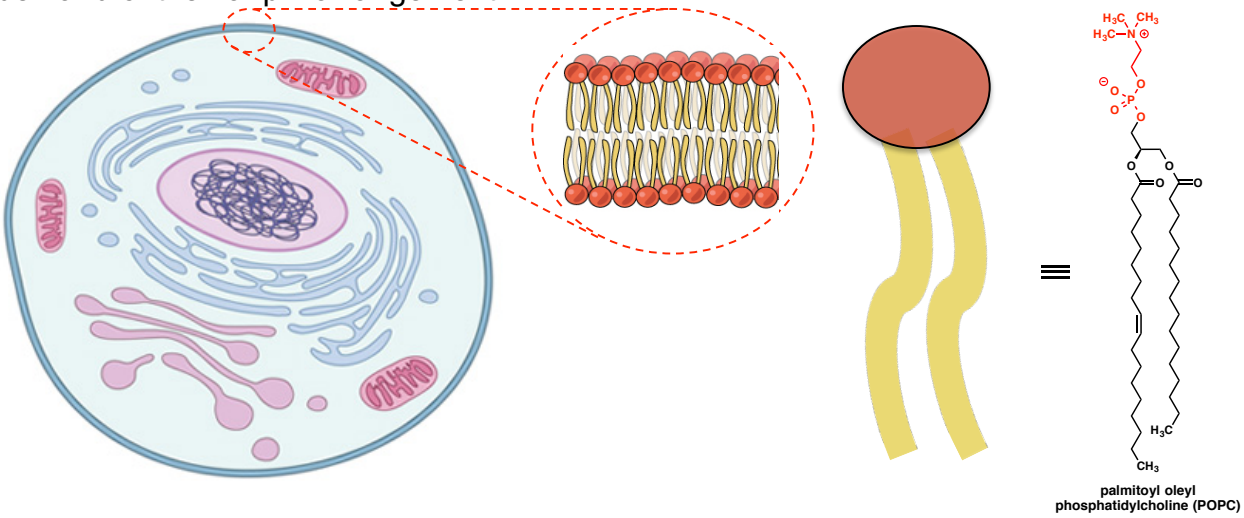

Figure 1. Canonical membrane structure and lipid molecular structure.

Results

Interested in this phenomenon and curious about its implications for lipid biophysics, we initially aimed to corroborate the autoradiographic evidence—which relied on extensive fractionation[4]—with an *in situ* approach to show that chlorosulfolipids are indeed located in the membranes of *O. danica*. To this end, we selected nanoscale secondary ion mass spectrometry (NanoSIMS) imaging. In NanoSIMS, a primary beam bombards the surface of a sample with heavy ions and fragments the molecules in the sample. [6] These atomic and polyatomic fragments are then separated and detected with a mass spectrometer. By scanning the ion beam over the sample one pixel at a time and recording the counts for all ions of interest, one can simultaneously generate multiple ion-specific images of a single field of view. NanoSIMS images of 5 µm-thick sections of *O. danica* cells immobilized in gelatin and embedded in a water-soluble resin suggest enrichment of chlorine in cell membranes (Figure 3). Combined with the results of Haines et al.,[4] these data suggest that chlorosulfolipids may play a primary structural role in *O. danica* membranes.

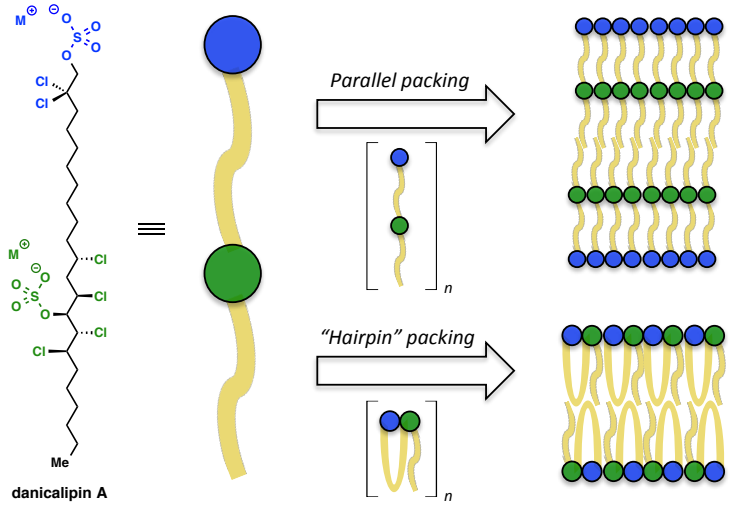

Figure 2. Hypothetical chlorosulfolipid membrane structure.

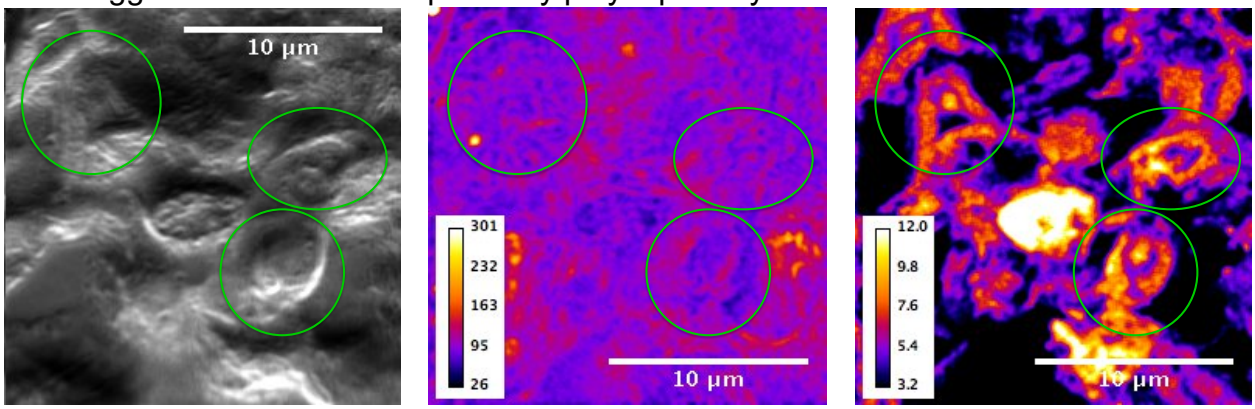

Secondary e⁻ ***$^{12}C^-$*** ***$^{35}Cl^- / {}^{12}C^-$ ratio***

Figure 3. NanoSIMS images of 5 µm-thick O. danica cross-sections.

The implication of the above data is that chlorosulfolipids can form a stable membrane. This would run counter to the observation by Vanderwal et al. that danicalipin A (Figure 2) is soluble in water, in contrast to canonical membrane lipids which readily form turbid suspensions.[5] One hypothesis reconciling these concepts is that the presence of some stabilizing positively charged element absent in water, such as a protein residue,[5] inorganic cation (M^+ in Figure 2),[5] or hydronium ion[7] allows the formation of a chlorosulfolipid bilayer. To investigate the possibility of ion-induced membrane formation, we hydrated dried films of synthetic danicalipin A[8] and used dynamic light scattering (DLS) to measure the sizes of particles formed upon hydration and the intensity of light scattered by the samples (Figure 4). Although salts had a flocculating effect, Ca^{2+} had a dramatic effect on the apparent turbidity of the suspension, suggesting that Ca^{2+} plays a stabilizing role in the formation of chlorosulfolipid

nanoparticles and supporting the hypothesis that divalent cations stabilize chlorosulfolipid membranes.

Encouraged by this result, we grew cultures of *O. danica* for rapid, large-scale access to >10 mg/batch quantities of danicalipin A for further studies. Fluorescence microscopy and cryotransmission electron microscopy (cryoTEM) were carried out on aqueous suspensions of extracted and purified danicalipin A[2] to characterize the light-scattering particles. On a fluorescence microscope, it quickly became apparent that hydrated suspensions of danicalipin A contained only particles that were below the diffraction limit in size (Figure 5, left).

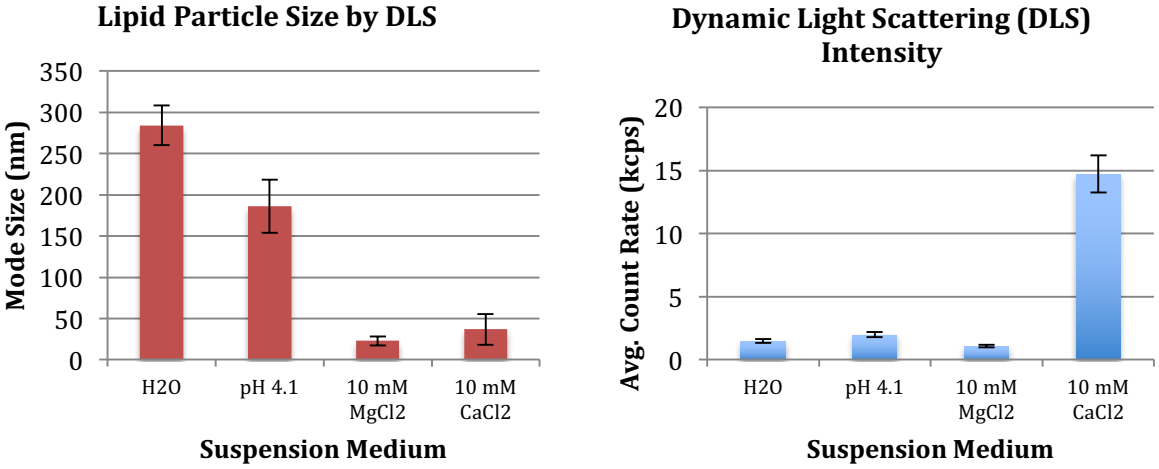

Figure 4. DLS data collected on suspensions of danicalipin A in aqueous solutions.

By cryoTEM, however, after extensive procedural optimization we were able to see apparently membranous disordered lipid (Figure 5, center) as well as rare apparently vesicular structures (Figure 5, right).

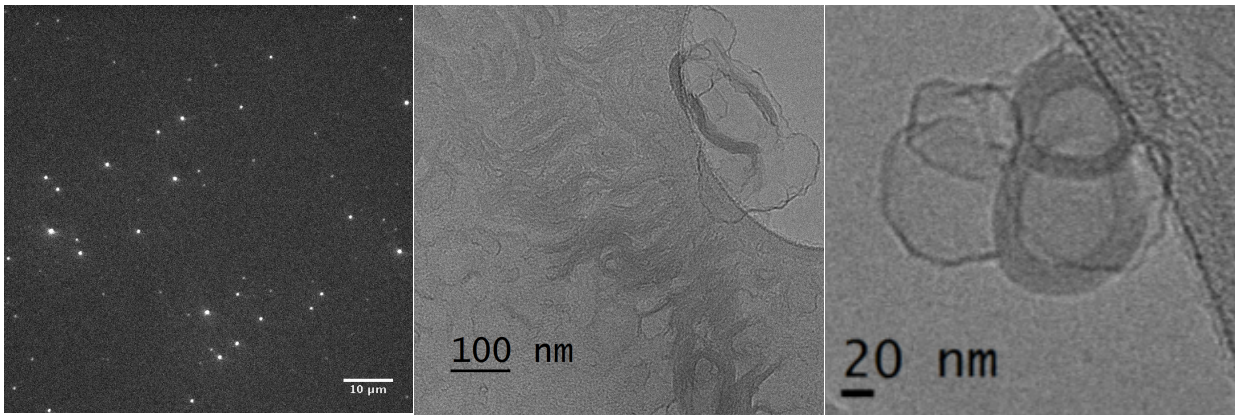

Figure 5. Left, fluorescence microscope image of danicalipin A in 10 mM $CaCl_2$ (DiI, 0.1 mol%). Center and right, cryoTEM images of danicalipin A in 10 mM $MgCl_2$.

Future directions

The ultimate question with a biomolecule as unusual as danicalipin A is that of function. Our plan since the start of this project has been to (1) prove that chlorosulfolipids are capable of self-assembling into stable membranes; (2) explain the physical basis for this stability; (3) probe the physical properties of chlorosulfolipid membranes to inform hypotheses about biological function; (4) perform biological studies that validate these hypotheses; and (5) take technological advantage of the chlorosulfolipid membranes' properties.

At this juncture, we are still in the pursuit of goals 1 and 2. In order to further prove that chlorosulfolipid membranes exist, a chlorosulfolipid-based system must be developed that can be imaged with high vesicular abundance; considering experimental challenges in accomplishing this goal with cryoTEM, a preparation of giant (>10 μm) vesicles would be ideal. In pursuit of this, we plan to perform traditional giant unilamellar vesicle (GUV) preparation techniques such as electroformation and gentle hydration on chlorosulfolipid-based systems, including mixtures of lipids with stabilizing elements such as sterols and glycolipids which are known to reside in the flagellar membrane alongside chlorosulfolipids.[4]

As far as membrane structure, molecular dynamics (MD)-based simulations in conjunction with Langmuir-Blodgett experiments on monolayers at the air-water interface and small-angle X-ray scattering (SAXS) studies on hydrated films are underway and are likely to inform us about the stability and structural nature of the chlorosulfolipid membrane. Following this probation of the chlorosulfolipid membrane structure, traditional membrane property charactization methods such as differential scanning calorimetry (DSC), fluorescence recovery after photobleaching (FRAP), transmembrane diffusion studies and lateral conductivity studies[9] will inform hypotheses regarding both biological function and potential technological utility.

3. Assignment of the absolute configuration of the anammox bacterial lipid tail [3]-ladderane.

Ladderane lipids, named for the ladder-like polycyclobutane motifs in their hydrophobic tails, are produced by anaerobic ammonium oxidizing (anammox) bacteria as a significant fraction of their membrane lipids.[10] In a large intracellular compartment called the anammoxosome, anammox bacteria couple ammonium and nitrite to produce dinitrogen as their principle source of energy. Experimental and computational evidence suggests that ladderane lipids form a densely packed membrane around the anammoxosome and serve to limit the transmembrane diffusion of toxic or valuable metabolites from anammox catabolism.

The ladderane structures likely impart a number of previously unobserved characteristics in membrane settings, but their biophysical characterization has been hampered by a lack of access to pure material. An axenic culture of anammox bacteria is not available, and growth rates of enrichment cultures in laboratory reactors are slow (doubling times on the order of 1−2 weeks). Furthermore, anammox bacteria produce an array of ladderane and nonladderane lipids, which have proven inseparable on a preparative scale. To circumvent these difficulties, researchers in the Burns lab designed a synthetic route that allows access to any ladderane lipid.

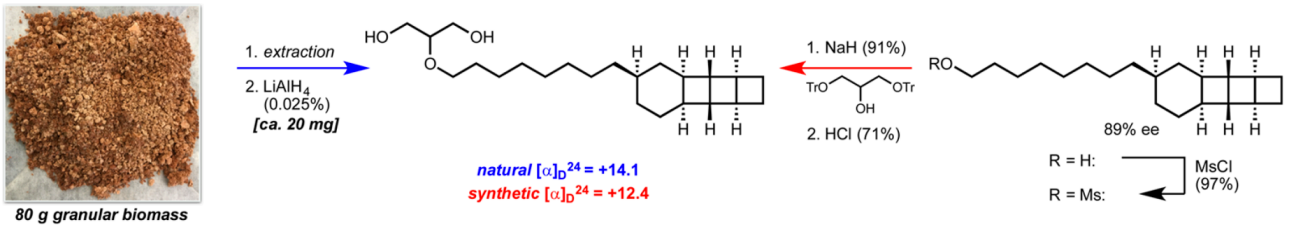

Scheme 2. Absolute configuration of [3]-ladderane.

The glycerol stereocenter of ladderane phospholipids has been established to be (R), which is consistent with other prokaryotic membrane phospholipids. However, the absolute stereochemistry of the ladderane tails has remained unknown. With the goal of completing this assignment, I conducted a lipid extraction of biomass from an anammox enrichment culture grown over four months in a laboratory-scale bioreactor. Cognizant that [3]-ladderane glycerol diol (Scheme 2, top) is one of the most readily separable components of ladderane lipid mixtures, I treated the crude extracts directly with lithium aluminum hydride to reduce all ester and phosphoester linkages and enrich for [3]-ladderane. From 80 g of dried biomass, I obtained a sufficient amount of [3]-ladderane for an optical rotation ([α]D = +14.1). Synthetic [3]-ladderane prepared via alkylation of bis-tritylglycerol with [3]-ladderanol mesylate was also found to be dextrorotatory ([α]D = +12.4 at 88% ee), which established the natural configuration of [3]-ladderane as drawn.

Natural [5]-ladderane alcohol from our extracts was inseparable from the corresponding [3]-ladderane alcohol and other straight-chain lipid alcohols. To the best of our knowledge, natural [5]-ladderane, first characterized as its methyl ester, has never been completely separated from contaminating [3]-ladderane methyl ester, which makes synthesis the only way to obtain pure [5]-ladderane lipids. We have assumed by analogy to that the configuration of natural [5]-ladderane is analogous.

4. Development and usage of a hydrazine transmembrane diffusion assay using a new synthetic fully water-soluble hydrazine sensor for biophysical evidence of the function of ladderane lipids in nature.

INTRODUCTION

Lipid membranes are universal features of living systems. Along with membrane proteins, they form the internal and peripheral barriers of cells and organelles and maintain non-equilibrium states necessary for life. Cells produce a diverse array of lipid structures and expend considerable energy to tightly control the lipid compositions of their membranes.[11] In conventional phospholipid bilayers, it is known that longer hydrocarbon tails and fewer degrees of unsaturation reduce fluidity and slow lateral diffusion, as well as affect phase behavior of *in vitro* model membranes (Fig. 6a).[12,13] However, there exist natural membrane lipids with unusual hydrophobic tail structures and in most cases the physical properties and biological functions of lipids with such structures are unexplored.

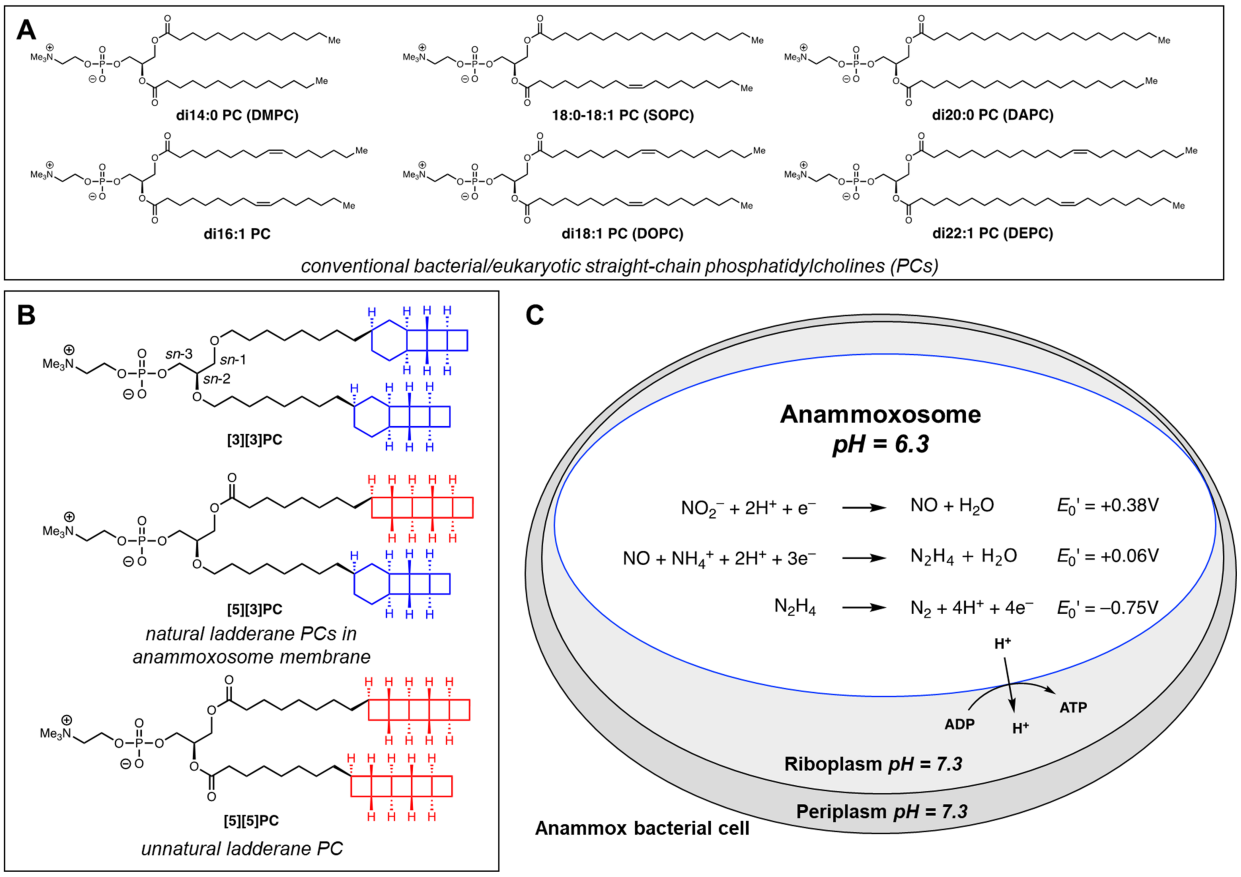

Figure 6. Lipid structures and anammox metabolism. (A) Representative straight-chain PCs. Nomenclature: x:y is a straight chain with x carbons and y degrees of unsaturation. (B–C) Ladderane lipids such as [3][3]PC and [5][3]PC occur naturally in the anammoxosome membrane of anammox bacteria. (B) Naturally occurring [3][3]PC and [5][3]PC phospholipids and unnatural analogue [5][5]PC that have been prepared by enantioselective chemical synthesis. (C) Anammox catabolism is believed to provide energy to the cell by oxidizing the toxic intermediate hydrazine (N_2H_4). Hydrazine oxidation is thought to be coupled to proton influx, generating a pH gradient that drives ATP synthesis.

The ladderane lipids, comprised of fatty lipid tails terminating in either a [3]-ladderane motif (highlighted in blue in Fig. 6B) or a [5]-ladderane motif (highlighted in red in Fig. 6B), occur uniquely in anaerobic ammonium oxidizing (anammox) bacteria and are some of the most structurally exotic lipids known.[14,15] Typically, natural ladderane phospholipids have a 20-

carbon [3]-ladderane ether linked at the *sn*-2 position of a glycerol backbone.[16,17,18,19] Substitution at the *sn*-1 position varies widely and includes ether- or ester-linked ladderane, linear, and branched hydrocarbon tails of varying lengths. Anammox bacteria are not yet available as a pure culture, and anammox enrichment cultures grow very slowly (doubling times on the order of 1–2 weeks).[20,21] Isolation of lipids from anammox enrichment cultures yields a complex and practically inseparable mixture, which prevents biophysical characterization of individual ladderane species.[22,23] To enable experiments on ladderane lipids with complete control over structure, we developed *de novo* enantioselective chemical syntheses of both [3]- and [5]-ladderane lipid tails and a small set of ladderane phospholipids.[24] As a representative sample of natural ladderane phospholipids, we prepared a [5]-ladderane-[3]-ladderane phosphatidylcholine (**[5][3]PC**, Fig. 6B) and a di-[3]-ladderane phosphatidylcholine (**[3][3]PC**, Fig. 6B), two of the most common ladderane phospholipids across a range of anammox genera.[18] Additionally, we prepared di-[5]-ladderane phosphatidylcholine (**[5][5]PC**, Fig. 6B), which is not known to occur naturally.

Ladderanes are enriched in the membrane of the anammoxosome, a specialized organelle within which anammox catabolism is thought to occur.[14] Ammonium and nitrite are coupled to produce dinitrogen via intermediate hydrazine (N_2H_4); oxidation of hydrazine to dinitrogen is highly exergonic, and this free energy is believed to be harnessed to pump protons across the anammoxosome membrane.[25,26,27] The resulting pH gradient of approximately 1 unit in turn powers ATP synthesis (Fig. 6C).[28,29,30] Hydrazine's cellular toxicity and bioenergetic value as a metabolic intermediate have led to the hypothesis that ladderanes serve to prevent the diffusion of hydrazine out of the anammoxosome, thereby protecting the contents of the riboplasm and periplasm from free hydrazine while preserving metabolic energy.[14,30] It has also been reasoned, based on long anammox doubling times and slow hydrazine synthase activity, that ladderanes might prevent the passive diffusion of protons out of the anammoxosome (although the directionality of the pH gradient has not been experimentally determined) in order to preserve the proton motive force necessary for ATP synthesis.[14,31] Another theoretical study suggests ladderanes might trap reactive species such as free radicals in addition to protons.[32] Although studies on enrichment cultures and lipid extracts suggest that the anammoxosome membrane is dense and relatively impermeable to dyes, hypotheses about hydrazine and proton permeability remain to be experimentally tested.[14,22]

We recently completed the total synthesis of a pure ladderane phospholipid, which we expand in this work to a total of three phospholipids with distinct tail structures for structure-function studies.[24] Biophysical experiments on model membranes composed of these synthetic lipids allow us to identify properties of individual molecular ladderane species for the first time. We disclose that ladderane phospholipid bilayers exhibit normal hydrazine permeability, but low proton/hydroxide permeability. It should be noted that our model membranes do not contain the proteins nor the entire variety of lipids observed in anammox lipid extracts, which may affect these properties in anammox membranes.[16]

RESULTS

Syntheses of Ladderane PCs

We recently reported enantioselective total syntheses of a [5]-ladderane fatty acid and a [3]-ladderane fatty alcohol.[24] These lipid tails were then elaborated to **[5][3]PC**, **[3][3]PC**, and **[5][5]PC** using a modification of our previously reported phosphatidylcholine synthetic route (Supplementary Schemes 1–3).

Differential Scanning Calorimetry (DSC)

Lipid films were hydrated with a low-melting and high-boiling 1:1 ethylene glycol/phosphate buffer mixture, and DSC was performed to measure the transition temperature (T_m) of the multilamellar lipid dispersions. Control experiments showed that the effect of ethylene glycol on T_m is negligible. A single transition between –40 and 80 °C was observed for each ladderane PC. The presence of a [3]-ladderane tail at the *sn*-2 position apparently ensures a low transition temperature (compare **[5][3]PC**, T_m = 11.8 ºC to **[5][5]PC**, T_m = 68.4 ºC, Fig. 7A). We believe the cyclohexane ring in the [3]-ladderane motif introduces a kink in the lipid tail, mirroring the fluidizing effect of *cis*-unsaturation in the *sn*-2 position tail of a straight chain lipid (compare 18:0-18:1 PC (SOPC), T_m = 4.1 ºC to di18:0 PC (DSPC), T_m = 57.1 ºC). **[5][5]PC** has approximately the same T_m as di20:0 PC (DAPC), whereas **[3][3]PC** has a T_m similar to di22:1 PC (DEPC).

A

Lipid	T_m (°C)
di18:2 PC	-52.7 ± 1.6
di16:1 PC	-33.0 ± 0.1
di18:1 PC (DOPC)	-10.9 ± 0.1
16:0-18:1 PC (POPC)	-4.8 ± 0.1
18:0-18:1 PC (SOPC)	4.1 ± 0.1
di22:1 PC (DEPC)	15.8 ± 0.1
di14:0 PC (DMPC)	24.3 ± 0.1
di18:0 PC (DSPC)	57.1 ± 0.1
di20:0 PC (DAPC)	67.8 ± 0.1
[5][3]PC	11.8 ± 0.2
[3][3]PC	15.2 ± 0.1
[5][5]PC	68.4 ± 0.1

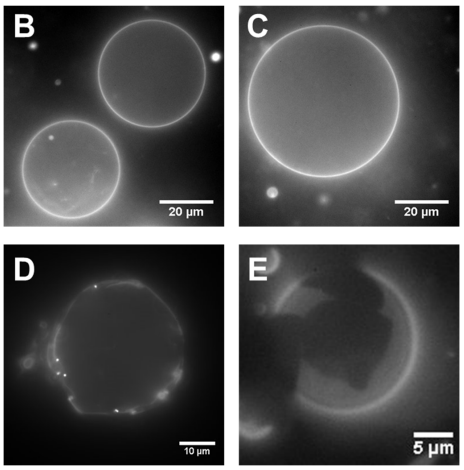

Figure 7. Transition temperatures and formation of giant unilamellar vesicles. (A) Transition temperatures (T_m) of aqueous lamellar dispersions of PCs in 1:1 ethylene glycol/NaH_2PO_4 buffer measured by DSC. (B–E) Fluorescence microscope images of giant unilamellar vesicles (GUVs) (TR-DHPE or DiI, 0.1 mol%) in 500 mM sucrose. For additional images see Supplementary Fig. 3. (B) [3][3]PC, (C) [5][3]PC, (D) [5][5]PC, (E) 1:1 [3][3]PC:[5][5]PC.

Self-Assembly of Ladderane Phospholipids into Lipid Bilayers

We next evaluated whether ladderane PCs would self- assemble into giant unilamellar vesicles (GUVs) using established methods.[33, 34, 35] Upon gentle hydration, films of **[3][3]PC** and **[5][3]PC** appeared to form GUVs (Figs. 7B–C) with homogeneous incorporation of dye (0.1 mol% Texas Red-DHPE (TR-DHPE) or DiI) and spherical shapes confirming that these lipids form fluid bilayers at room temperature. Formation of GUVs from **[5][5]PC** required heating above its T_m, and upon cooling we observed fluorescent objects similar to gel-phase GUVs formed from DAPC (Fig. 7D). A 1:1 mixture of **[3][3]PC** and **[5][5]PC** formed GUVs with visible domains that exclude both TR-DHPE (Fig. 7E) and DiI (not shown) in a manner analogous to mixtures of straight-chain phospholipids that form bilayers with coexisting phases at room temperature.[36,37]

Hydration of **[3][3]PC** or **[5][3]PC** films followed by extrusion through a 50 nm-pore polycarbonate membrane resulted in the formation of small unilamellar vesicles (SUVs) of similar light scattering intensity and polydispersity to those formed from common PCs, albeit of about 20% larger average size (120-122 nm vs. 92-98 nm). However, ladderane SUVs with the same size as straight-chain PC SUVs could be achieved with a more rigorous extrusion protocol (98 nm).

Hydrazine Transmembrane Diffusion Assay

To test the hypothesis that ladderanes form a barrier to transmembrane diffusion of hydrazine, we developed an assay based on a small molecule sensor that fluoresces upon condensation with hydrazine.[38] Preparation of a derivative with added hydrophilic sulfonate and amide groups was necessary to improve aqueous solubility and presumably reduce interactions between the dye and the membrane; the final hydrazine sensor (**HS**)-based hydrazine transmembrane diffusion kinetic assay design is illustrated in Fig. 8A.[39] We also confirmed that HS does not localize in lipid bilayers.

We performed this hydrazine diffusion assay on SUVs composed of several straight-chain PCs, **[3][3]PC**, and **[5][3]PC**. SUVs encapsulating **HS** in a pH = 7.4 phosphate buffer were added to an equiosmolar pH = 7.4 buffer containing hydrazine, and changes in the fluorescence intensity were measured over time (Fig. 8B). Among straight-chain PCs, hydrazine transmembrane diffusion rates depended strongly on hydrophobic tail length (Fig. 8C), likely due to different bilayer thicknesses among these lipids.[40,41,42] SUVs of ladderane PCs exhibited half-lives ($t_{1/2}$'s) of hydrazine transmembrane diffusion well within the range exhibited by SUVs of straight-chain PCs. We have also conducted this diffusion assay at the anammoxosome-relevant pH of 6.3 with SOPC, DEPC, and **[3][3]PC**. Transmembrane diffusion rates are all slower, as expected, but maintain the same trend as at pH = 7.4.

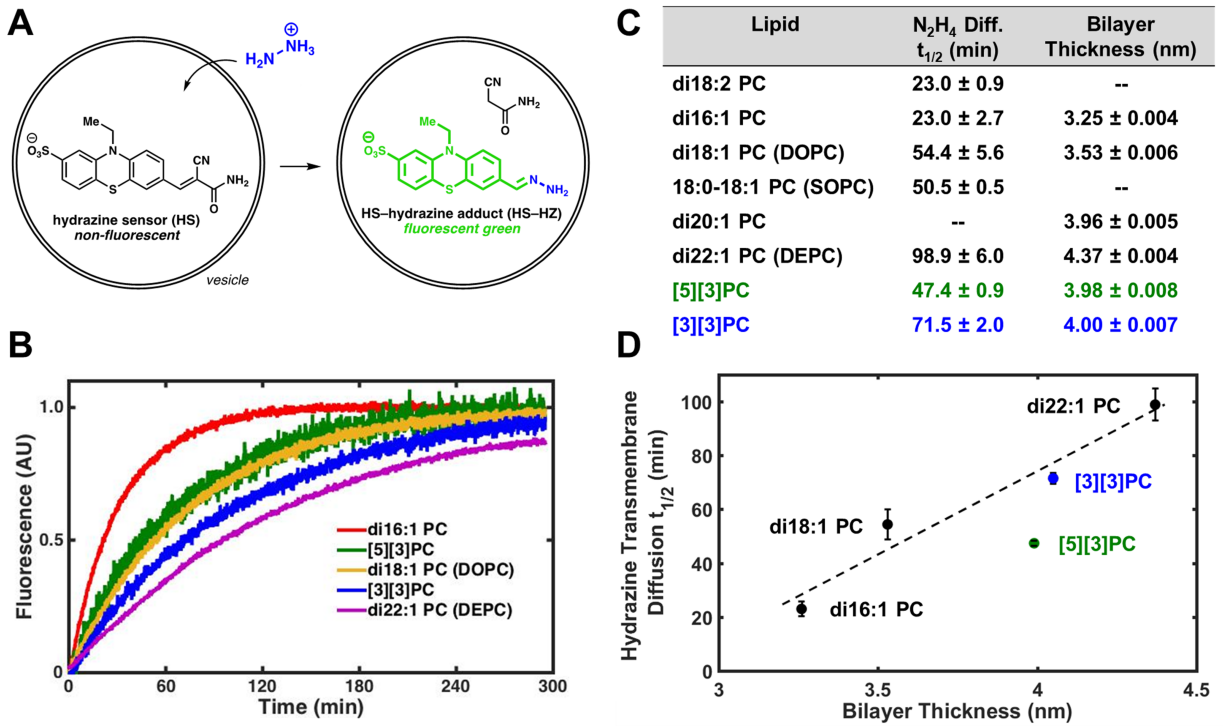

Lipid	N_2H_4 Diff. $t_{1/2}$ (min)	Bilayer Thickness (nm)
di18:2 PC	23.0 ± 0.9	--
di16:1 PC	23.0 ± 2.7	3.25 ± 0.004
di18:1 PC (DOPC)	54.4 ± 5.6	3.53 ± 0.006
18:0-18:1 PC (SOPC)	50.5 ± 0.5	--
di20:1 PC	--	3.96 ± 0.005
di22:1 PC (DEPC)	98.9 ± 6.0	4.37 ± 0.004
[5][3]PC	47.4 ± 0.9	3.98 ± 0.008
[3][3]PC	71.5 ± 2.0	4.00 ± 0.007

Figure 8. Hydrazine transmembrane diffusion assay and bilayer thickness as estimated by small-angle X-ray scattering (SAXS). (A) Illustration of N_2H_4 transmembrane diffusion assay using a new water-soluble derivative (HS) of a fluorogenic hydrazine sensor. (B) Hydrazine transmembrane diffusion curves for representative straight-chain and ladderane PCs. (C) Table of hydrazine transmembrane diffusion half-lives and bilayer thicknesses. (D) Hydrazine transmembrane diffusion half-life versus bilayer thickness. Dashed line illustrates linear correlation for di16:1 PC, di18:1 PC, di22:1 PC, and [3][3]PC.

Small-Angle X-Ray Scattering (SAXS). To examine the relationship between hydrazine diffusion rate and bilayer thickness, we performed small angle X-ray scattering on rigorously extruded SUVs of unsaturated straight-chain PCs and ladderane PCs (Fig. 8C). Bilayers of straight-chain PCs increased in thickness with increasing chain length from 3.25 nm for di16:1 PC to 4.37 nm for di22:1 PC.

The [3]-ladderane and [5]-ladderane tails in our synthetic ladderane phospholipids each contain 20 carbons, and **[3][3]PC** and **[5][3]PC** formed bilayers of about the same thickness as di20:1 PC (~ 4 nm). SAXS curves also confirmed the high level of unilamellarity of SUVs.

pH Equilibration Across Membranes

To test the hypothesis that ladderanes form a barrier to transmembrane diffusion of protons/hydroxide ions, we performed a carboxyfluorescein (CF)-based assay of pH equilibration (Fig. 9A) on SUVs of several straight-chain PCs, **[3][3]PC**, and **[5][3]PC**.[43] SUVs encapsulating CF at pH = 7.2 in bis-tris propane buffer were added to equiosmolar pH = 5.8 bis-tris propane buffer, creating a transmembrane pH gradient that spontaneously decayed over time. The decrease in CF fluorescence was used to monitor the decrease in pH inside the SUVs as protons/hydroxide ions equilibrated across the bilayers. We also performed control experiments with valinomycin to confirm that a buildup of membrane potential was not affecting relative pH equilibration rates and with gramicidin to confirm that vesicles were unilamellar. We confirmed that valinomycin inserts into ladderane bilayers with the fluorescent K^+ sensor PBFI.[44] Equilibration of pH across **[3][3]PC** and **[5][3]PC** bilayers was approximately an order of magnitude slower than across membranes composed of straight-chain PCs (48-75 min vs. 0.33-6.9 min $t_{1/2}$) (Figs. 9B–C). We observe a correlation between T_m and pH equilibration $t_{1/2}$ for straight-chain PCs; however, **[5][3]PC** and **[3][3]PC** deviate strongly from this trend, suggesting that unique intermolecular interactions between ladderane lipid tails affect rates of pH equilibration (Fig. 9D).

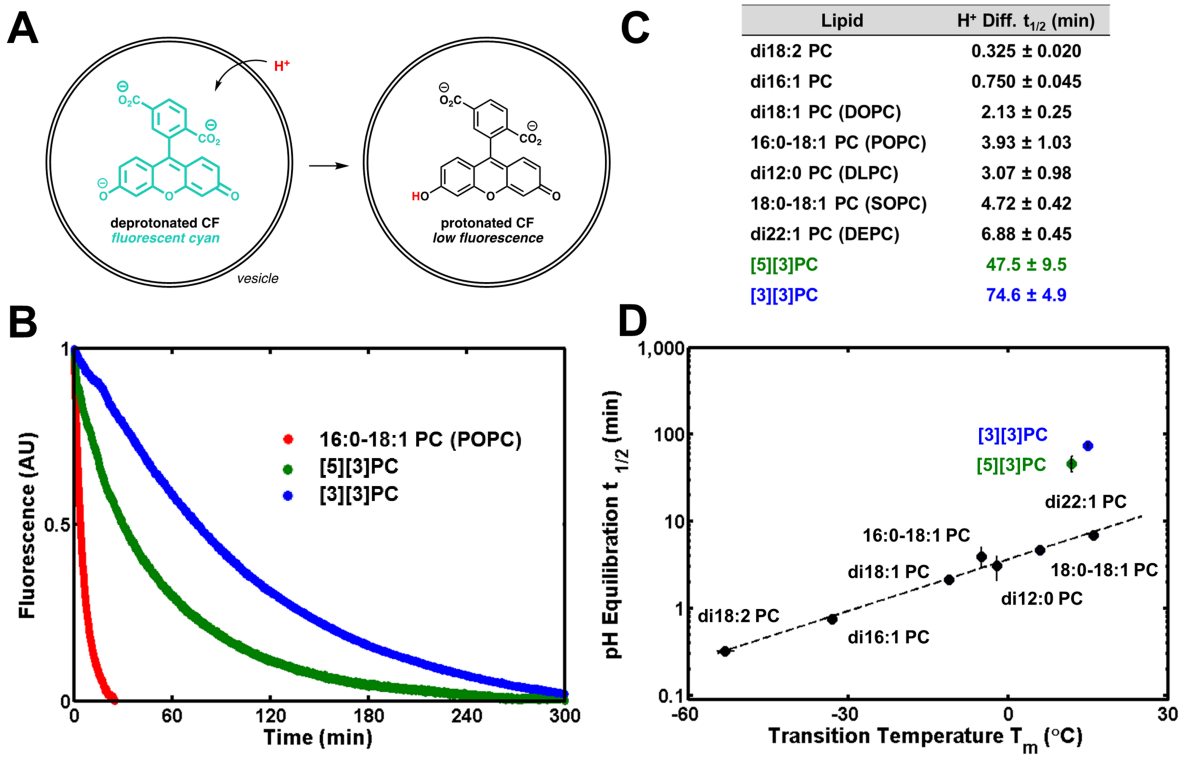

Lipid	H^+ Diff. $t_{1/2}$ (min)
di18:2 PC	0.325 ± 0.020
di16:1 PC	0.750 ± 0.045
di18:1 PC (DOPC)	2.13 ± 0.25
16:0-18:1 PC (POPC)	3.93 ± 1.03
di12:0 PC (DLPC)	3.07 ± 0.98
18:0-18:1 PC (SOPC)	4.72 ± 0.42
di22:1 PC (DEPC)	6.88 ± 0.45
[5][3]PC	47.5 ± 9.5
[3][3]PC	74.6 ± 4.9

Figure 9. pH equilibration assay. (A) Illustration of assay: influx of protons into (or efflux of hydroxide from) vesicles results in the protonation of CF, resulting in a decrease in fluorescence intensity. (B) Kinetic curves show that equilibration of pH across ladderane PC bilayers is much slower than across straight-chain PC bilayers, as illustrated by the case of POPC. (C) Table of pH equilibration half-lives $t_{1/2}$. (D) The logarithm of pH equilibration $t_{1/2}$ and straight-chain PC T_m are correlated, while ladderane PCs deviate from this trend.

Pressure-Area Isotherms of Langmuir Monolayers

To help explain the low proton/hydroxide permeability of ladderane PC bilayers, we investigated the physical properties of PC monolayers at the air-water interface. Monolayers provide an experimentally tractable model for investigating some properties of lipid bilayers. Ladderane PC monolayers collapse at surface pressures similar to liquid-phase monolayers of POPC (Fig. 10a), yet their compressibilities, *C,* are similar to those of solid-phase monolayers of DAPC (Fig.10C). In addition, monolayers of ladderane phospholipids have mean molecular areas (MMAs) smaller than fluid straight-chain PCs (Fig. 5C). These data suggest that at room temperature the ladderane PC monolayers exist in a phase that is fluid but more tightly packed than straight-chain PCs. Pressure-area isotherms for **[5][3]PC** and **[3][3]PC** are qualitatively similar to the previously published isotherm for a ladderane PC mixed extract.[22]

Fluorescence Recovery After Photobleaching (FRAP)

To quantitate fluidity in ladderane PC bilayers, we performed FRAP experiments on glass-supported lipid bilayers (SLBs) using Oregon Green-DHPE (OG-DHPE) as a fluorescent probe (Fig. 10B). As expected for lipids in a gel phase at room temperature, SLBs of **[5][5]PC** showed no lateral diffusion (Fig. 10B). SLBs of **[5][3]PC** and **[3][3]PC** exhibited lateral diffusion coefficients, *D*, at least one order of magnitude lower than SLBs of straight-chain PCs (0.24-0.29 $\mu m^2/s$ vs. 2.73-3.93 $\mu m^2/s$) (Figs. 10B-C). Straight-chain PCs show a linear correlation between *D* and T_m while ladderane PCs deviate strongly from this trend (Fig. 10D), further corroborating distinct physical properties for these unusual lipids.

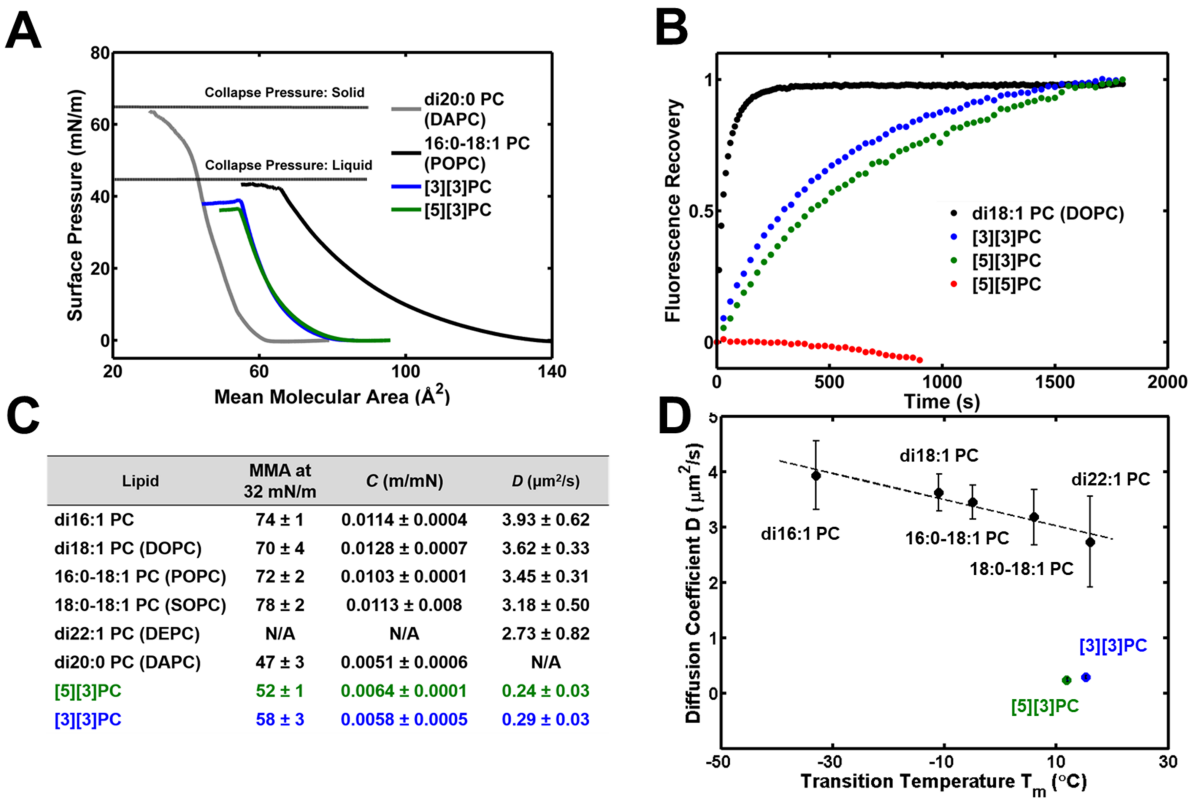

Lipid	MMA at 32 mN/m	*C* (m/mN)	*D* (μm²/s)
di16:1 PC	74 ± 1	0.0114 ± 0.0004	3.93 ± 0.62
di18:1 PC (DOPC)	70 ± 4	0.0128 ± 0.0007	3.62 ± 0.33
16:0-18:1 PC (POPC)	72 ± 2	0.0103 ± 0.0001	3.45 ± 0.31
18:0-18:1 PC (SOPC)	78 ± 2	0.0113 ± 0.008	3.18 ± 0.50
di22:1 PC (DEPC)	N/A	N/A	2.73 ± 0.82
di20:0 PC (DAPC)	47 ± 3	0.0051 ± 0.0006	N/A
[5][3]PC	52 ± 1	0.0064 ± 0.0001	0.24 ± 0.03
[3][3]PC	58 ± 3	0.0058 ± 0.0005	0.29 ± 0.03

Figure 10. Biophysical studies on PC monolayers and bilayers. (A) Pressure-area isotherms on Langmuir monolayers composed of di20:0 PC (DAPC, T_m = 68 °C), 16:0-18:1 PC (POPC, T_m = –4.8 °C), and ladderane PCs (T_m = 12–15 °C). (B) Fluorescence recovery after photobleaching (FRAP) curves of ladderane PCs and a representative straight-chain PC, di18:1 PC (DOPC). (C) Physical parameters extracted from isotherms and FRAP curves. MMA, mean molecular area (Å²); *C*, compressibility; *D*, lateral diffusion coefficient. (D) *D* correlates linearly with T_m for straight-chain PCs, but ladderane PCs deviate from this trend with diffusion coefficients approximately an order of magnitude lower.

DISCUSSION

Although much work has been done to understand the permeability of membranes to easily detectable drugs and organic dyes, methods of quantifying transmembrane diffusion of small hydrophilic molecules such as hydrazine in real-time are limited.[45] Early examples include the use of radioactive isotopes, while more recent methods use indirect detection, such as a pH change resulting from NH_4^+ diffusion.[46,47,48] Additionally, hydrazine is not stable to oxygen, causing difficulties in *ex situ* analysis. **HS** offers an approach to detecting hydrazine *in situ*, enabling a reproducible hydrazine transmembrane diffusion assay that was not feasible using existing sensors. With the commercial availability of pure PCs with various hydrophobic tail structures and our total synthesis of ladderane PCs, we were able to study the effect of PC tail structure on hydrazine permeability.

The lack of correlation between the rates of pH equilibration and hydrazine transmembrane diffusion provides experimental evidence that these processes occur by different mechanisms. Evidence from the literature supports a model in which proton/hydroxide diffusion occurs via water molecules in the bilayer that act as proton wires or water clusters that carry protons.[30, 49 , 50 , 51 , 52] Transmembrane diffusion of other ions (e.g. K^+) and small neutral molecules (e.g. H_2O, O_2, CO_2), the rates of which are directly dependent on bilayer thickness, is thought to occur via direct partitioning into the bilayer and diffusion through the hydrophobic region of the bilayer.[53,21] Our data are consistent with the idea that this is the case for hydrazine. As described in the Results section, our data do not support the hypothesis that ladderane PCs alone offer any advantage with respect to hydrazine permeability. Ladderane PC bilayers and straight-chain PC bilayers have similar rates of hydrazine transmembrane diffusion. Notably, the relative hydrazine permeability of ladderane bilayers compared to conventional PC bilayers was correctly predicted by molecular dynamics simulations.[54]

In contrast, equilibration of pH across the **[3][3]PC** bilayer was at least 10 times slower than across bilayers composed of any straight-chain PC. To the best of our knowledge this is the slowest known pH equilibration to be measured across a homogeneous PC bilayer, although very slow pH equilibration across archaea-inspired tetraether lipid monolayers is also known.[33] Rates of pH equilibration for straight-chain PC bilayers correlate strongly with their T_ms. A lipid's T_m reflects the strength of intermolecular interactions and lipid packing. Our data are consistent with a model in which water must disrupt lipid-lipid interactions in the fluid phase in order to form a proton-conductive wire or cluster in the hydrophobic region of the bilayer. For straight-chain PCs these interactions are accurately reflected in the T_ms, but this correlation breaks down with **[3][3]PC** and **[5][3]PC**. Monolayers of **[3][3]PC** and **[5][3]PC** at room temperature have smaller MMAs and lower compressibilities than fluid straight-chain PC monolayers, suggesting tighter packing and a higher level of molecular order in the fluid bilayer that is somehow not reflected in the T_m. However, these stronger intermolecular interactions are reflected in the slower lateral diffusion rates in SLBs. Finally, it is interesting to note that **[3][3]PC** and **[5][3]PC**, which each have 20-carbon ladderane tails, form bilayers of similar thickness to di20:1 PC, indicating that the conformational rigidity of the polycyclobutane ladderane motifs counterbalances their shortened structure for a null net effect on bilayer thickness.

Our data provide sufficient information to build a qualitative model for ladderane bilayer structure. From a broad structural perspective, bilayers of naturally occurring ladderane PCs are more densely packed than bilayers of straight-chain PCs, while still remaining fluid at room temperature. High London dispersion interactions between ladderane hydrocarbons have been predicted computationally.[55] The strong ladderane-ladderane interactions might resist the formation of a proton-conductive water cluster/wire, which would disrupt these

interactions.[45,49,51,52] This is consistent with the very low *D* of ladderane bilayers, as this same disruption of packing is necessary for the OG-DHPE to diffuse laterally. *D* correlates well with pH equilibration $t_{1/2}$ for all PCs assessed, including ladderanes, indicating that *D* reports on the strength of the physical interactions relevant to proton/hydroxide permeability (Supplementary Fig. 22). Hydrazine, which is much smaller than a water cluster or an OG-DHPE molecule, may be able to diffuse through small, transient spaces without wholly disrupting ladderane-ladderane packing.[22,56]

CONCLUSIONS

The facile preparation of vesicles, monolayers, and supported bilayers of **[3][3]PC** and **[5][3]PC** was not anticipated, as their unique structural elements might be expected to alter their molecular spontaneous curvature and favor non-bilayer structures. However, this self-assembly is consistent with the observation that ladderanes are the primary lipid components of the membranes in anammox bacteria, suggesting a major structural role for ladderane phospholipids. Anammox bacteria rely on a pH gradient to drive ATP synthesis.[29,30] Loss of this pH gradient during the slow anammox metabolism would make this process unviable as a source of energy for the cell. Our data support the hypothesis that ladderanes evolved at least in part to impede the loss of this vital pH gradient.

The use of pure ladderane PCs, both natural and unnatural, has allowed us to explore structure-function relationships and develop a physical understanding of ladderane phospholipid bilayers at a molecular level of detail which was not previously accessible. This was enabled by the success of a scalable natural product total synthesis.[24] Our biophysical results are qualitatively similar to results from complex mixtures of ladderanes, but we are able to observe functional distinctions between individual molecules that are lost in mixtures.[22,23] Chemical synthesis also enabled the development of a fluorogenic sensor-based hydrazine permeability assay, the results of which suggest that the unique ladderane lipids have little effect on transmembrane hydrazine diffusion. Hydrazine containment by other means, such as rapid conversion within the hydrazine synthase complex or retention within encapsulin nanocompartments, remains a possibility.[27,57] The results that ladderane PCs form bilayers with normal hydrazine permeability and anomalously low proton/hydroxide permeability served as an impetus for Langmuir monolayer analysis and FRAP experiments that point to the possible origin of this property, i.e. dense packing of the ladderanes. This packing has been suggested and hypothetically tied to both proton and hydrazine permeability by others.[14,30,31] Herein, we provide experimental evidence suggesting that limiting proton/hydroxide permeability is one of the primary purposes of ladderanes in anammox bacterial membranes. More generally, we have demonstrated that lipid packing in the hydrophobic region of the lipid bilayer can strongly affect the permeability of the bilayer to small ions. Cells may utilize this mechanism to control the permeabilities of their membranes.

The complexity and biological relevance of our system could be increased by including hopanoid terpenes, natural ladderane/branched-chain hybrid lipids, and various phospholipid headgroups that are also found in the anammoxosome membrane.[16,17,18] A better understanding of the quantitative compositions of the different membranes of anammox bacteria would guide these studies. Additionally, it may be possible and useful to reconstitute membrane proteins in ladderane membranes to study ladderane-protein interactions, or to study membrane protein functions that depend on pH gradients that are rapidly lost with conventional phospholipids.

5. References.

[1] Haines, T. H. Sulfolipids and Halosulfolipids. In *Lipids and Biomembranes of Eukaryotic Microorganisms*; Academic Press: New York, 1973; pp 197-232.
[2] Kawahara, T.; Kumaki, Y.; Kamada, T.; Ishii, T.; Okino, T. *J. Org. Chem.* **2009**, *74*, 6016–6024.
[3] Mercer, E. I.; Davies, C. L. *Phytochemistry* **1979**, *18*, 457–462.
[4] Chen, L. L.; Pousada, M.; Haines, T. H. *J. Biol. Chem.* **1976**, *251*, 1835–1842.
[5] Bedke, D. K.; Vanderwal, C. D. *Nat. Prod. Rep.* **2011**, *28*, 15–25.
[6] Boxer, S. G.; Kraft, M. L.; Weber, P. K. *Annu. Rev. Biophys.* **2009**, *38*, 53–74.
[7] Haines, T. H. Personal correspondence.
[8] Landry, M. L.; Hu, D. X.; McKenna, G. M.; Burns, N. Z. *J. Am. Chem. Soc.* **2016**, *138*, 5150–5158.
[9] Cevc, G.; et al. *Biophysical J.* **1995**, *69*, 489–497.
[10] Mercer, J. A. M.; Cohen, C. M.; Shuken, S. R.; Wagner, A. M.; Moss, F. R.; Boxer, S. G.; Burns, N. Z.; et al. *J. Am. Chem. Soc.* **2016**, *138*, 15845–15848.
[11] van Meer G, Voelker DR, Feigenson GW (2008) Membrane lipids: where they are and how they behave. *Nat Rev Mol Cell Biol* 9(2):112–124.
[12] Alberts B, Johnson A, Lewis J, Raff M, Roberts K, Walter P (2008) Membrane Structure. *Molecular Biology of the Cell* (Garland Science, New York), pp 617–650.
[13] Simons K, Vaz WLC (2004) Model Systems, Lipid Rafts, and Cell Membranes. *Ann Rev Biophys Biomol Struct 33*:269–295.
[14] Sinninghe Damsté, JS, Strous M, Rijpstra IC, Hopmans EC, Geenevasen JAJ, van Duin ACT, van Niftrik LA, Jetten MSM (2002) Linearly concatenated cyclobutane lipids form a dense bacterial membrane. *Nature* 419(6908):708–712.
[15] Nouri DH, Tantillo DJ (2006) They Came From the Deep: Syntheses, Applications, and Biology of Ladderanes. *Curr Org Chem* 10(16):2055−2075.
[16] Sinninghe Damsté JS, Rijpstra WIC, Geenevasen JAJ, Strous M, Jetten MSM (2005) Structural identification of ladderane and other membrane lipids of planctomycetes capable of anaerobic ammonium oxidation (anammox). *FEBS J* 272(16):4270–4283.
[17] Boumann HA, Hopmans EC, van de Leemput I, Op den Camp HJM, van de Vossenberg J, Strous M, Jetten MSM, Sinninghe Damsté JS, Schouten S (2006) Ladderane phospholipids in anammox bacteria comprise phosphocholine and phosphoethanolamine headgroups. *FEMS Microbiol Lett* 258(2):297–304.
[18] Rattray JE, van de Vossenberg J, Hopmans EC, Kartal B, van Niftrik L, Rijpstra WIC, Strous M, Jetten MSM, Schouten S, Sinninghe Damsté JS (2008) Ladderane lipid distribution in four genera of anammox bacteria. *Arch Microbiol* 190(1):51–66.
[19] Sinninghe Damsté, JS, Rijpstra WIC, Strous M, Jetten MSM, David ORP, Geenevasen JAJ, van Maarseveen JH (2004) A mixed ladderane/*n*-alkyl glycerol diether membrane lipid in an anaerobic ammonium-oxidizing bacterium. *Chem Commun* (22):2590–2591.
[20] Strous M, Heijnen JJ, Kuenen JG, Jetten MSM (1998) The sequencing batch reactor as a powerful tool for the study of slowly growing anaerobic ammonium-oxidizing microorganisms. *Appl Microbiol Biotechnol* 50(5):589–596.
[21] van der Star WRL, Miclea AI, van Dongen UG, Muyzer G, Picioreanu C, van Leesdrecth MCM (2008) The Membrane Bioreactor: A Novel Tool to Grow Anammox Bacteria as Free Cells. *Biotechnol Bioeng* 101(2):286–294.
[22] Boumann HA, Longo ML, Stroeve P, Poolman B, Hopmans EC, Stuart MCA, Sinninghe Damsté JS, Schouten S (2009) Biophysical properties of membrane lipids of anammox bacteria: I. Ladderane phospholipids form highly organized fluid membranes. *Biochim Biophys Acta* 1788(7):1444–1451.
[23] Boumann HA, Stroeve P, Longo ML, Poolman B, Kuiper JM, Hopmans EC, Jetten MSM, Sinninghe Damsté JS, Schouten S (2009) Biophysical properties of membrane lipids of anammox bacteria: II. Impact of temperature and bacteriohopanoids. *Biochim Biophys Acta* 1788(7):1452–1457.

[24] Mercer JAM, Cohen CM, Shuken SR, Wagner AM, Smith MW, Moss FR, III, Smith MD, Vahala R, Goncalez-Martinez A, Boxer SG, Burns NZ (2016) Chemical Synthesis and Self-Assembly of a Ladderane Phospholipid. *J Am Chem Soc* 138(49):15845–15848.
[25] Kuenen JG (2008) Anammox bacteria: from discovery to application. *Nat Rev Microbiol* 6(4):320–326.
[26] Kartal B, Maalcke WJ, de Almeida NM, Cirpus I, Gloerich J, Geerts W, Op den Camp HJM, Harhangi HR, Janssen-Megens EM, Francoijs K-J, Stunnenberg HG, Keltjens JT, Jetten MSM, Strous M (2011) Molecular mechanism of anaerobic ammonium oxidation. *Nature* 479(7371), 127–130.
[27] Dietl A, Ferousi C, Maalcke WJ, Menzel A, de Vries S, Keltjens JT, Jetten MSM, Kartal B, Barends TRM (2015) The inner workings of the hydrazine synthase multiprotein complex. *Nature* 527(7578):394–397.
[28] Van der Star WRL, Dijkema C, de Waard P, Picioreanu C, Strous M, van Loosdrecht MCM (2010) An intracellular pH gradient in the anammox bacterium *Kuenenia stuttgartiensis* as evaluated by 31P NMR. *Appl Microbiol Biotechnol* 86(1):311–317.
[29] van Niftrik LA, Fuerst JA, Sinninghe Damsté JS, Kuenen JG, Jetten MSM, Strous M (2004) The anammoxosome: an intracytoplasmic compartment in anammox bacteria. *FEMS Microbiol Lett* 233(1):7–13.
[30] Kartal B, de Almeida NM, Maalcke WJ, Op den Camp HJM, Jetten MSM, Keltjens JT (2013) How to make a living from anaerobic ammonium oxidation. *FEMS Microbiol Rev* 37(3):428–461.
[31] Jetten MSM, van Niftrik L, Strous M, Kartal B, Keltjens JT, Op den Camp HJM (2009) Biochemistry and molecular biology of anammox bacteria. *Crit Rev Biochem Mol Biol* 44(2-3):65–84.
[32] Nouri DH, Tantillo DJ (2012) Attack of radicals and protons on ladderane lipids: quantum chemical calculations and biological implications. *Org Biomol Chem* 10(29):5514-5517.
[33] Reeves JP, Dowben RM (969) Formation and properties of thin-walled phospholipid vesicles. *J Cell Physiol* 73(1):49–60.
[34] Walde P, Cosentino K, Engel H, Stano P (2010) Giant vesicles: preparations and applications. *ChemBioChem* 11(7):848-865.
[35]Akashi K, Miyata H, Itoh H, Kinosita K (1996) Preparation of giant liposomes in physiological conditions and their characterization under an optical microscope. *Biophys J* 71(6):3242-3250.
[36] Feigenson GW, Buboltz JT (2001) Ternary Phase Diagram of Dipalmitoyl-PC/Dilauroyl-PC/Cholesterol: Nanoscopic Domain Formation Driven by Cholesterol. *Biophys J* 80(6):2775–2788.
[37] Veatch SL, Keller SL (2003) Separation of Liquid Phases in Giant Vesicles of Ternary Mixtures of Phospholipids and Cholesterol. *Biophys J* 85(5):3074–3083.
[38] Sun M, Guo J, Yang Q, Xiao N, Li Y (2014) A new fluorescent and colorimetric sensor for hydrazine and its application in biological systems. *J Mater Chem B* 2:1846–1851.
[39] Hughes LD, Rawle RJ, Boxer SG (2014) Choose Your Label Wisely: Water-Soluble Fluorophores Often Interact with Lipid Bilayers. *PLoS One* 9(2):e87649.
[40] Walter A, Gutknecht J (1986) Permeability of Small Nonelectrolytes through Lipid Bilayer Membranes. *J Membr Biol* 90(3):207–217.
[41] Lorent HJ, Levental I (2015) Structural determinants of protein partitioning into ordered membrane domains and lipid rafts. *Chem Phys Lipids* 192:23–32.
[42] Pignataro MF, Dodes-Traian MM, González-Flecha FL, Sica M, Mangialavori IC, Rossi JPFC (2015) Modulation of Plasma Membrane Ca^{2+}-ATPase by Neutral Phospholipids: effect of the micelle-vesicle transition and the bilayer thickness. *J Biol Chem* 290(10):6179–6190.
[43] Koyanagi T, Leriche G, Onofrei D, Holland GP, Mayer M, Yang J (2016) Cyclohexane Rings Reduce Membrane Permeability to Small Ions in Archaea-Inspired Tetraether Lipids. *Angew Chem Int Ed* 55(5):1890–1893.
[44] Hervé M, Cybulska, B, Gary-Bobo CM (1985) Cation permeability induced by valinomycin, gramicidin D and amphotericin B in large lipidic unilamellar vesicles studied by ^{31}P-NMR. *Eur Biophys J* 12(3):121–128.

[45] Liu H, Sabus C, Carter GT, Du C, Avdeef A, Tischler M (2003) *In Vitro* Permeability of Poorly Aqueous Soluble Compounds Using Different Solubilizers in the PAMPA Assay with Liquid Chromatography/Mass Spectrometry Detection. *Pharm Res* 20(11):1820–1826.
[46] Papahadjopoulos D, Jacobson K, Nir S, Isac T (1973) Phase transitions in phospholipid vesicles: Fluorescence polarization and permeability measurements concerning the effect of temperature and cholesterol. *Biochim Biophys Acta* 311(3):330–348.
[47] Bangham AD, Standish MM, Watkins JC (1965) Diffusion of Univalent Ions across the Lamellae of Swollen Phospholipids. *J Mol Biol* 13(1):238–252.
[48] Mathai JC, Sprott GD, Zeidel ML (2001) Molecular Mechanisms of Water and Solute Transport across Archaebacterial Lipid Membranes. *J Biol Chem* 276(29):27266–27271.
[49] Paula S, Deamer DW (1999) Membrane Permeability Barriers to Ionic and Polar Solutes. *Curr Top Membr* 48:77–95.
[50] Deamer DW, Nichols JW (1999) Proton Flux Mechanisms in Model and Biological Membranes. *J Membr Biol* 107(2):91–103.
[51] Marrink SJ, Jähnig F, Berendsen HJC (1996) Proton Transport across Transient Single-File Water Pores in a Lipid Membrane Studied by Molecular Dynamics Simulations. *Biophys J* 71(2):632–647.
[52] Tepper HL, Voth GA (2005) Protons May Leak through Pure Lipid Bilayers via a Concerted Mechanism. *Biophys J* 88(5):3095-3108.
[53] Mathai JC, Tristram-Nagle S, Nagle JF, Zeidel ML (2008) Structural Determinants of Water Permeability through the Lipid Membrane. *J Gen Physiol* 131(1):69–76.
[54] Chaban VV, Nielsen MB, Kopec W, Khandelia H (2014) Insights into the role of cyclic ladderane lipids in bacteria from computer simulations. *Chem Phys Lipids* 181:76–82.
[55] Wagner JP, Schreiner PR (2014) Nature Utilizes Unusual High London Dispersion Interactions for Compact Membranes Composed of Molecular Ladders. *J Chem Theory Comput* 10(3):1353–1358.
[56] Paula S, Volkov AG, Van Hoek AN, Haines TH, Deamer DW (1996) Permeation of protons, potassium ions, and small polar molecules through phospholipid bilayers as a function of membrane thickness. *Biophys J* 70(1):339–348.
[57] Giessen TW, Silver PA. Widespread distribution of encapsulin nanocompartments reveals functional diversity. *Nature Microbiol* 2:1–11.